

## An improved numerical simulator for multiphase flow in porous media

I. Garrido<sup>\*,†</sup>, G. E. Fladmark and M. Espedal

*Department of Mathematics, University of Bergen, Johannes Bruns gt. 12, N-5008 Bergen, Norway*

### SUMMARY

In basin modelling the thermodynamics of a multicomponent multiphase fluid flux are computationally too expensive when derived from an equation of state and the Gibbs equality constraints. In this article we present a novel implicit molar mass formulation technique using binary mixture thermodynamics. The two proposed solution methods, with and without cross derivative terms between components, are based on a preconditioned *Newton-GMRES* scheme for each time-step with analytical computation of the derivatives. These new algorithms reduce significantly the numerical effort for the computation of the molar masses, and we illustrate the behavior of these methods with numerical computations. Copyright © 2004 John Wiley & Sons Ltd.

KEY WORDS: compositional simulator; multiphase flow; Newton-GMRES; binary mixture thermodynamics

### 1. INTRODUCTION

The primary objective of basin simulation is to determine the possible locations of trapped hydrocarbons. Since the hydrocarbons use millions of years to migrate, the basin structure may change several times during the migration. It is not only the geometry and the geological data which cause difficulties. Compared to a reservoir model, a basin model includes many more unknowns due to the heat transport, chemical reactions and thermodynamics. Our work is based on a compositional simulator for secondary oil migration [1–4]. This 3D model gives full treatment of fractures and discontinuities of the medium, representing them by refined cells which contain the desired lithology [5–7].

In this work we have mostly used a simplified compositional model, named the binary mixture thermodynamics model [8]. The phase calculation is related to tables for dew and bubble points rather than fugacity calculations. In this model the oil and the gas components may partly be in both the oil and gas phases, while the water phase is treated separately.

---

\*Correspondence to: I. Garrido, Department of Mathematics, University of Bergen, Johannes Bruns gt. 12, N-5008 Bergen, Norway.

†E-mail: izaskun@mi.uib.no

The primary variables in our simulator, named Athena, are the temperature,  $T$ , the water pressure,  $p^w$ , and the molar masses,  $N_v$ , for each fluid component,  $v$ . The numerical model uses a control volume finite difference box-centred space discretization technique together with a *backward Euler* scheme for time discretization of the water pressure and temperature equations and an *explicit* solver for the mass equation. Recently a *fixed LGR* method has been successfully applied to cover discontinuities of the porous media [9]. This method does not only allow a full geometrical treatment of fault and matrix but it also serves as a middle step between the sequential and parallel processing, see References [10, 11] for a comparison with other simulators. Obviously, the above discretization introduces a CFL condition that severely restricts the time step [12]. In order to avoid the time step restriction imposed from the CFL condition, we propose two implicit numerical schemes which deal with the mass conservative dynamical behavior while reducing the numerical effort.

The main goal of this article is to present an implicit formulation and illustrate the efficiency of the simulator with the new methods by numerical examples. For that purpose we consider different geometries and compare the numerical results obtained by the two implicit algorithms, based on a *preconditioned Newton-GMRES* [13] with analytical derivatives, to those obtained by the *explicit* solver. For further information on Krylov subspace methods we refer to the classical paper from Saad [14] and specific applications to oil reservoirs [15]. For further details about basin modelling we refer the interested reader to References [16–20].

An outline of the paper is as follows: in Section 2 we introduce the model to study. The numerical approximations to the primary variables temperature, water pressure and molar mass are given in Sections 3–5, respectively. The entries for the Jacobians in the two implicit molar mass transport formulations are derived in Section 6; other discretization schemes are given in References [21–23]. Then, in Section 7, we present some numerical results, and conclusions and future work summarize the paper in Section 8.

## 2. THE MODEL

In this section we will give an introduction to the simulation model, which is implemented into the general compositional simulator Athena. It is based on the symmetric black oil model with the assumption that the water is always in water phase and any of the hydrocarbons may be in both gas and oil phase. For more information and details about compositional models we refer to References [24–26].

For consistency reasons we introduce the following notation; the sub index  $v$  will denote any of the  $n_c$  fluid components, while the super index  $l$  denotes any of the three phases, oil, water or gas, in which the different components or fraction of them may exist. The water component is assumed to always be in water phase whilst the hydrocarbons are never in water phase. Besides, discretization indices will appear between brackets as subindices for the space and as super-indices for the time.

The molar mass conservation of a multicomponent multiphase fluid flow flowing through a porous media region,  $V$ , whose boundary is a closed surface,  $S$ , is given by the integral expression

$$\frac{\partial}{\partial t} \int_V m_v dV + \int_V \nabla \cdot \mathbf{m}_v = - \int_V q_v dV \quad (1)$$

Here  $q_v$  denotes the source/sink of molar mass density for each component  $v$  with units mol/m<sup>3</sup>s. Besides, the molar mass flux and the density inside the region are respectively expressed as

$$\mathbf{m}_v = \sum_{l=\text{phase}} C_v^l \mathbf{v}^l \zeta^l \tag{2}$$

$$m_v = \phi_p \sum_{l=\text{phase}} C_v^l S^l \zeta^l \tag{3}$$

The entity  $C_v^l$  denotes the mass fraction of component  $v$  in phase  $l$ , and further  $\zeta^l = \rho^l/M^l$  the molar density of phase  $l$ ,  $\rho^l$  the mass density of phase  $l$ ,  $M^l$  the molecular weight of phase  $l$ ,  $S^l$  the saturation of phase  $l$ ,  $\mathbf{v}^l$  the Darcy velocity of phase  $l$ , and  $\phi_p$  the rock porosity.

Energy conservation is enforced by the following integral expression for the heat flow equation

$$\frac{\partial}{\partial t} \int_V (\rho u) dV - \int_S (\underline{k} \nabla T) d\mathbf{S} = - \int_S h \rho \mathbf{u} d\mathbf{S} + \int_V q dV \tag{4}$$

where the capacity term and convective flux are

$$\rho u = \sum_{l=g,o,w} \phi_p S^l u^l \rho^l + u_r \rho_r (1 - \phi_p) \tag{5}$$

$$h \rho \mathbf{u} = \sum_{l=g,o,w} h^l \rho^l \mathbf{v}^l \tag{6}$$

Here, the new parameters denote  $T$  the temperature,  $\underline{k}$  the bulk heat conductivity,  $\rho_r$  mass density of rock,  $u_r$  internal energy of rock,  $u^l$  internal energy of phase  $l$ , and  $h^l$  enthalpy of phase  $l$ .

The Volume Balance method [27] imposes that the difference between the pore volume,  $V_p$ , and the volume of all phases

$$R = V_p - \sum_{l=g,o,w} V^l \tag{7}$$

has to be zero at any time. Besides, this residual volume is a function of the water pressure,  $p^w$ , the overburden pressure,  $W$ , and the integral of the molar mass for each component,  $N_v$ . Hence, the first order Taylor expansion of the residual  $R(t + \Delta t)$  together with the chain rule for partial differentiation of  $\partial R(p^w, W, N_v)/\partial t$  leads to the water pressure equation

$$\frac{\partial R}{\partial p^w} \frac{\partial p^w}{\partial t} + \sum_{v=1}^{n_c} \frac{\partial R}{\partial N_v} \frac{\partial N_v}{\partial t} = - \frac{R}{\Delta t} - \frac{\partial R}{\partial W} \frac{\partial W}{\partial t} \tag{8}$$

In what follows, the numerical model will be derived from the discretization of the conservation equations (1), (4) and (8), using control volumes in space [28] together with backward Euler in time.

## 3. ENERGY CONSERVATION

The integral of the source term of Equation (4) will be treated explicitly for each control volume  $V_{[i]}$

$$\int_{V_{[i]}} q \, dV \approx Q_{[i]} \quad (9)$$

Since the convective flux, given by Equation (6), is small compared to the conductive flux, this term may be neglected or treated explicitly, in which case, the integral over each of the boundary surfaces is approximated by the value at the upstream control volume. Denoting by  $I(i)$  the set of indices for the upstream volume  $V_i$ , the convective flux of Equation (4) may be discretized as

$$\sum_k \int_{S_{[i,k]}} h \rho \mathbf{u} \, d\mathbf{S} \approx \Phi, \quad \Phi_{[i]} = \sum_{in \in I(i)} \sum_{l=g,o,w} h_{[i]}^l \rho_{[i]}^l \mathbf{v}_{[in]}^l S_{[i,k(in)]} \quad (10)$$

where  $S_{[i,k]}$  denotes the  $k$ th part of the surface boundary of the  $i$ th control volume, and  $S_{[i,k(in)]}$  the part of the surface between the  $i$ th and  $in$ th control volumes.

The conductive heat flow for the  $i$ th control volume is approximated by

$$\int_{S_{[i]}} (k \nabla T) \, d\mathbf{S} \simeq - \sum_{j \in \mathcal{M}_i} \alpha_{[ij]} T_{[j]} \quad (11)$$

where  $\alpha_{[ij]}$  are the conductivity coupling coefficients, and the set  $\mathcal{M}_i$  consists of the indices for all neighbors of the  $i$ th control volume including itself.

Finally, the capacity term is a function of the temperature

$$\frac{\partial}{\partial t} \int_V (\rho u) \, dV \simeq \int_V \frac{\partial}{\partial t} (\rho u) \, dV \simeq \int_V \left( \delta \frac{\partial T}{\partial t} \right) \, dV \quad (12)$$

where

$$\delta = \sum_{l=g,o,w} \phi_p S^l c^l \rho^l + c_r \rho_r (1 - \phi_p) \quad (13)$$

The term  $c_r = \partial h_r / \partial T$  denotes the rock specific heat capacity and  $c^l = \partial h^l / \partial T$  the specific heat capacity of the phases. Even when the creation or disappearance of phases within each control volume may provoke large changes per phase, one would expect a more linear and smooth behavior over the addition of all phases. Space discretization is done by cell centred finite difference approximation, using an explicit value for the heat capacity at each centre of the control volumes

$$\frac{\partial}{\partial t} \int_{V_{[i]}} (\rho u) \, dV \simeq \delta_{[i]} \frac{\partial T_{[i]}}{\partial t} \quad (14)$$

We have therefore substituted Equations (9)–(11) and (14) into Equation (4) to obtain the following finite control volume discretization of the energy

$$\delta_{[i]} \frac{\partial T_{[i]}}{\partial t} + \sum_{j \in \mathcal{M}_i} \alpha_{[ij]} T_{[j]} = -\Phi_{[i]} + Q_{[i]} \quad (15)$$

which together with a backward Euler time discretization leads to a residual equation with matrix notation

$$0 = \mathcal{D}(\mathbf{T}^{[n+1]}) \frac{\mathbf{T}^{[n+1]} - \mathbf{T}^{[n]}}{\Delta t^{[n]}} + \mathcal{A}(\mathbf{T}^{[n+1]})\mathbf{T}^{[n+1]} - \mathbf{b}(\mathbf{T}^{[n]}) \tag{16}$$

Here,  $\Delta t^{[n]} = t^{[n+1]} - t^{[n]}$ ,  $\mathcal{D} = \text{diag}(\delta_{[i]})$ ,  $\mathcal{A} = (\alpha_{[ij]})$  and  $\mathbf{b} = (Q_{[i]} - \Phi_{[i]})$ . Besides, both the convection and conduction terms have coefficients dominated by the rock temperature, which is almost constant, so that this equation may be linearized as

$$\mathcal{J}^{[n]} \Delta \mathbf{T}^{[n]} = -\mathbf{f}^{[n]} \tag{17}$$

where  $\Delta \mathbf{T}^{[n]} = (\mathbf{T}^{[n+1]} - \mathbf{T}^{[n]})$  and

$$\mathcal{J}^{[n]} = \frac{\mathcal{D}^{[n]}}{\Delta t^{[n]}} + \mathcal{A}^{[n]}, \quad \mathbf{f}^{[n]} = \mathcal{A}^{[n]}\mathbf{T}^{[n]} - \mathbf{b}^{[n]} \tag{18}$$

#### 4. TREATMENT OF THE WATER PRESSURE EQUATION

Space discretization for the integral of Equation (8) is done by the simple centred control volume evaluation

$$\delta_{[i]} \frac{\partial P_{[i]}^w}{\partial t} + \sum_{v=1}^{n_c} \varepsilon_{v,[i]} \frac{\partial N_{v,[i]}}{\partial t} = s_{[i]} \tag{19}$$

where

$$\delta_{[i]} = \left( \frac{\partial R}{\partial p^w} \right)_{[i]}, \quad \varepsilon_{v,[i]} = \left( \frac{\partial R}{\partial N_v} \right)_{[i]} \tag{20}$$

and  $s_{[i]}$  denotes the value of the right hand side of Equation (8) at the centre of the  $i$ th control volume.

In the discrete equation (19), the molar mass derivative may be expressed in terms of the water pressure. This approximation is obtained from Equation (1), which using the divergence theorem reads

$$\frac{\partial N_v}{\partial t} + \int_S \sum_{l=\text{phase}} C_v^l \zeta^l \mathbf{v}^l \cdot \mathbf{n} \, dS = Q_v \tag{21}$$

where  $\mathbf{n}$  is the unit outward normal vector to the boundary surface  $S$ , and  $Q_v$  is the integral of the source term for component  $v$ . Using the following expression for the Darcy velocity for phase  $l$ :

$$\mathbf{v}^l = - \sum_{m=g, o, w} \frac{K}{\mu^m} \frac{k_r^{lm}}{\mu^m} (\nabla p^m - \gamma^m \nabla d) \tag{22}$$

with  $k_r^{lm}$  the generalized relative permeability for coupled multiphase flow,  $K$  the absolute permeability tensor,  $\mu^m$  viscosity of the phase  $m$ ,  $p^m$  fluid pressure of phase  $m$ ,  $\gamma^m$  specific

weight of phase  $m$ ,  $d$  the depth, and the transmissibility tensors of each chemical component  $v$  are

$$t_v^m = \sum_{l=g,o,w} C_v^{l,zl} \underline{K} \frac{k_r^{lm}}{\mu^m} \quad (23)$$

Hence, the molar mass derivative given in Equation (21) may be rewritten as

$$\frac{\partial N_v}{\partial t} = \int_S \sum_{m=g,o,w} t_v^m (\nabla p^m - \gamma^m \nabla d) \cdot \mathbf{n} dS + Q_v \quad (24)$$

Besides, the water pressure has been chosen as a primary variable so that the oil and gas phase pressures are given in terms of the water and the capillary pressures as

$$p^o = p^w + p_c^{ow}, \quad p^g = p^o + p_c^{og} \quad (25)$$

and part of the conductivity term is

$$\sum_{m=g,o,w} t_v^m \nabla p^m = \sum_{m=g,o,w} t_v^m \nabla p^w + (t_v^o + t_v^g) \nabla p_c^{ow} + t_v^o \nabla p_c^{og} \quad (26)$$

Evaluation at the centre of each control volume of the expression that results from substituting Equation (26) into Equation (24) leads to

$$\begin{aligned} \frac{\partial N_{v[i]}}{\partial t} &= \sum_{j \in \mathcal{M}_i} t_{v[ij]} p_{[j]}^w + \Psi_{v[i]} \\ \Psi_{v[i]} &= \sum_{j \in \mathcal{M}_i} ((t_{v[ij]}^g + t_{v[ij]}^o) p_{c[j]}^{ow} + t_{v[ij]}^g p_{c[j]}^{og} - g_{v[ij]} d_{[j]}) + Q_{v[i]} \end{aligned} \quad (27)$$

where  $t_{v[ij]} = \sum_l t_{v[ij]}^l$  denotes the discrete transmissibilities and  $g_{v[ij]}$  the equivalent discrete gravitation. Substituting the molar mass derivative approximation given by Equation (27) into Equation (19) gives at each control volume

$$\delta_i \frac{\partial P_{[i]}^w}{\partial t} + \sum_{j \in \mathcal{M}_i} \alpha_{[ij]} p_{[j]}^w = \beta_{[i]} \quad (28)$$

with

$$\alpha_{[ij]} = \sum_{v=1}^{n_c} \varepsilon_{v[i]} t_{v[ij]}, \quad \beta_{[i]} = s_{[i]} - \sum_{v=1}^{n_c} \varepsilon_{v[i]} \Psi_{v[i]} \quad (29)$$

Backward Euler time discretization of Equation (28) gives a residual matrix equation for the water pressure

$$\mathcal{J}(\mathbf{p}^{w[n+1]}) \frac{\mathbf{p}^{w[n+1]} - \mathbf{p}^{w[n]}}{\Delta t^{[n]}} + \mathcal{A}(\mathbf{p}^{w[n+1]}) \mathbf{p}^{w[n+1]} - \mathbf{b}(\mathbf{p}^{w[n+1]}) = 0 \quad (30)$$

with  $\Delta t^{[n]} = t^{[n+1]} - t^{[n]}$ . When solving this non-linear equation with the *Newton–Raphson* method, we ensure that  $\mathbf{p}^{w[n(k)]} \rightarrow \mathbf{p}^{w[n+1]}$  when  $k \rightarrow \infty$ , if our initial guess is ‘good’ enough. Then, by using Taylor expansion of order one at  $\mathbf{p}^{w[n(k)]} + \Delta \mathbf{p}^{w[n(k)]}$  we get the following equation for the increment

$$\mathcal{J}^{[n(k)]} \Delta \mathbf{p}^{w[n(k)]} = -\mathbf{f}^{[n(k)]} \quad (31)$$

where  $n(k)$  denotes the  $k$ th non-linear *Newton–Raphson* iteration at the  $n$ th time level

$$\mathcal{J}^{[n(k)]} = \left( \frac{\partial \mathbf{f}}{\partial \mathbf{p}^w} \right)^{[n(k)]} \simeq \frac{\mathcal{D}^{[n(k)]}}{\Delta t^{[n]}} + \mathcal{A}^{[n]}, \quad \Delta \mathbf{p}^{w[n(k)]} = \mathbf{p}^{w[n(k+1)]} - \mathbf{p}^{w[n(k)]} \quad (32)$$

and

$$\mathbf{f}^{[n(k)]} = \mathcal{D}^{[n(k)]} \frac{\mathbf{p}^{w[n(k)]} - \mathbf{p}^{w[n]}}{\Delta t^{[n]}} + \mathcal{A}^{[n]} \mathbf{p}^{w[n(k)]} - \mathbf{b}^{[n]}$$

Note that we do not update  $\mathcal{A}$  and  $\mathbf{b}$  for every iteration. The reason for this is that these calculations are rather expensive, and the accuracy we loose by this approximation may be neglected.

### 5. IMPLICIT MOLAR MASS EQUATIONS

Equation (1) is written as

$$\frac{\partial}{\partial t} N_v + \int_V \sum_l \nabla \cdot (C_v^l \xi^l \mathbf{v}^l) dV = Q_v \quad (33)$$

Since the molar mass of phase  $l$  is  $N^l = V^l \xi^l$ , and denoting the inverse of volume for phase  $l$  by  $a^l$ , Equation (33) may be now expressed as

$$\frac{\partial}{\partial t} N_v + \int_V \sum_l \nabla \cdot (C_v^l a^l N^l \mathbf{v}^l) dV = Q_v \quad (34)$$

Together with the divergence theorem, Equation (34) is equivalent to

$$\frac{\partial}{\partial t} N_v + \int_S \sum_l C_v^l a^l N^l \mathbf{v}^l \cdot \mathbf{n} dS = Q_v \quad (35)$$

where  $\mathbf{n}$  is the unit outward normal vector to the boundary surface  $S$ . This mass transport equation shall be rewritten in terms of the molar mass of component  $v$  in phase  $l$ ,  $N_v^l = C_v^l N^l$ , which leads to

$$\frac{\partial}{\partial t} N_v + \int_S \sum_l a^l N_v^l \mathbf{v}^l \cdot \mathbf{n} dS = Q_v \quad (36)$$

A finite control volume discretization is used to create the numerical model. Space discretization of Equation (36) is done by cell centred finite difference approximation. The flux term is considered to be continuous across interfaces of area  $A$ , so that the surface integral of the normal component at the boundary of a given volume may be discretized as

$$\frac{\partial}{\partial t} N_{v[i]} + \sum_{is \in S_i} \sum_l (a^l N_v^l)_{[in]} \theta_{[is]}^l = Q_{v[i]}, \quad \theta_{[is]}^l = (\mathbf{v}^l \cdot \mathbf{n})_{[is]} A_{[is]} \quad (37)$$

The index  $in$  denotes the upstream volume with respect to each interface,  $is$ , of the  $i$ th control volume.

Time discretization of Equation (37) is done by considering a backward Euler approximation of the derivative and by keeping the Darcy velocity and the phase volume constant at time  $t^{[n]}$

$$\frac{N_{v[i]}^{[n+1]} - N_{v[i]}^{[n]}}{\Delta t^{[n]}} + \sum_{is \in S_i} \sum_l (a^{l[n]} N_v^{l[n+1]})_{[in]} \theta_{[is]}^{l[n]} = Q_{v[i]}^{[n]} \quad (38)$$

where  $\Delta t^{[n]} = t^{[n+1]} - t^{[n]}$ . The advection term in Equation (38) will be treated implicitly when using *Newton–Raphson*. Thus, the molar mass of component  $v$  in phase  $l$  may be expanded in terms of the molar mass of the different components as

$$N_v^{l[n(k+1)]} = N_v^{l[n(k)]} + \sum_{\mu} \left( \frac{\partial N_v^l}{\partial N_{\mu}} \right)^{[n(k)]} \Delta N_{\mu}^{[n(k)]}, \quad \Delta N_{\mu}^{[n(k)]} = N_{\mu}^{[n(k+1)]} - N_{\mu}^{[n(k)]} \quad (39)$$

where  $N_v^{l[n(k)]} \rightarrow N_v^{l[n+1]}$  when  $k \rightarrow \infty$  and index  $n(k)$  denotes the  $k$ th non-linear *Newton–Raphson* iteration at the  $n$ th time level. Therefore, the discrete molar mass transport equation (38) of a chemical component  $v$  flowing through a porous media region of a closed surface  $S$ , may be rewritten as

$$\frac{\Delta N_{v[i]}^{[n(k)]}}{\Delta t^{[n]}} + \sum_{is \in S_i} \sum_l \left( a^{l[n]} \sum_{\mu} \left( \frac{\partial N_v^l}{\partial N_{\mu}} \right)^{[n(k)]} \Delta N_{\mu}^{[n(k)]} \right)_{[in]} \theta_{[is]}^{l[n]} = \beta_{v[i]}^{[n(k)]} \quad (40)$$

with right hand side

$$\beta_{v[i]}^{[n(k)]} = Q_{v[i]}^{[n]} - \frac{N_{v[i]}^{[n(k)]} - N_{v[i]}^{[n]}}{\Delta t^{[n]}} - \sum_{is \in S_i} \sum_l (a^{l[n]} N_v^{l[n(k)]})_{[in]} \theta_{[is]}^{l[n]} \quad (41)$$

### 5.1. Full Jacobian matrix formulation

Considering multicomponent multiphase fluid flow, the matrix formulation of the molar mass equilibrium discrete equation (40) is of the form

$$\left( \frac{\mathcal{I}}{\Delta t^{[n]}} + \mathcal{A}^{[n(k)]} \right) \Delta \mathbf{N}^{[n(k)]} = \mathbf{b}^{[n(k)]} \quad (42)$$

For a chemical system consisting of  $n_c$  components, located on a domain decomposed into  $n_{cv}$  control volumes

$$\begin{aligned} (\Delta \mathbf{N}^{[n(k)]})_{\mu_j} &= \Delta N_{\mu[j]}^{[n(k)]}, & (\mathbf{b}^{[n(k)]})_{v_i} &= \beta_{v[i]}^{[n(k)]} \\ v_i, \mu_j \in I, & I = \{(1, 1), \dots, (n_c, 1), \dots, (1, n_{cv}), \dots, (n_c, n_{cv})\} \end{aligned} \quad (43)$$

$\mathcal{I}$  is the identity matrix, and the matrix  $\mathcal{A}$  has been ordered in  $n_{cv}^2$  blocks each of them with  $n_c^2$  entries of the form

$$(\mathcal{A}^{[n(k)]})_{v_i, \mu_j} = \sum_l \alpha_{v_i, \mu_j}^{l[n(k)]} \quad (44)$$

where for given a phase  $l, j \in \text{Im}(i)$  denotes a cell which is upstream and  $i$  is the interface between cells  $i$  and  $j$

$$\alpha_{v_i, \mu_j}^{l[n(k)]} = 0, \quad j \notin \text{Im}(i) \quad \text{else} \quad \alpha_{v_i, \mu_j}^{l[n(k)]} = \alpha^{l[n]} \theta_{v[ij]}^{l[n]} (\partial N_v^l / \partial N_\mu)^{n(k)}_{[j]} \tag{45}$$

$$\alpha_{v_i, \mu_i}^{l[n(k)]} = - \sum_{j \in \text{Im}(i)} \alpha_{v_i, \mu_j}^{l[n(k)]}$$

5.2. Sequential matrix formulation

The discrete molar mass equation (40) may be simplified considering the cross-derivatives between different components to be negligible. This assumption eliminates the coupling and makes it possible to achieve greater computer efficiency by sequential solution of the following molar mass equations

$$\left( \frac{\mathcal{I}}{\Delta t^{[n]}} + \mathcal{A}_v^{[n(k)]} \right) \Delta \mathbf{N}_v^{[n(k)]} = \mathbf{b}_v^{[n(k)]}, \quad v = 1, \dots, n_c \tag{46}$$

where for a chemical system consisting of  $n_c$  components located on a domain decomposed into  $n_{cv}$  cells

$$(\Delta \mathbf{N}_v^{[n(k)]})_j = \Delta N_{v[j]}^{[n(k)]}, \quad (\mathbf{b}_v^{[n(k)]})_i = \beta_{v[i]}^{[n(k)]}, \quad i, j \in \{1, \dots, n_{cv}\} \tag{47}$$

$\mathcal{I}$  is the identity matrix and each matrix  $\mathcal{A}_v$  has  $n_{cv}^2$  entries  $(\mathcal{A}_v)^{[n(k)]}_{ij} = \sum_l \alpha_{v_i, v_j}^{l[n(k)]}$ , which are defined similarly to those of the full Jacobian.

Each set of Equations (17), (31) and (42) or (17), (31) and (46), results in a compact numerical model, since they allow to find all the primary and secondary variables for the new time step.

6. THREE PHASE SYSTEM

The partial molar mass derivatives which appear in the molar mass discrete equations (42) and (46) are approximated based on binary system thermodynamics. Roughly speaking, the flux has three components; water, oil and gas which may be in either water, oil or gas phase. In particular, the oil and gas components should be viewed as the hydrocarbon components of the flux lumped into one gas and one oil component. This approximation at any fixed time  $t$ , generates for each phase  $l = w, o, g$  the partial derivatives

$$\frac{\partial N_v^l}{\partial N_\mu}, \quad v, \mu = w, o, g \tag{48}$$

where  $v$  and  $\mu$  denote the lumped (grouped) components.

6.1. Single hydrocarbon phase state

The derivatives under consideration (48) depend on the number of phases that are present in a control volume at that time. The single phase generates two sub-cases corresponding to being either only oil phase present or only gas phase present

$$N^g = 0: \quad N^o = N_o + N_g; \quad N_o^o = N_o \quad \text{and} \quad N_g^o = N_g,$$

$N^o = 0$ :  $N^g = N_o + N_g$ ;  $N_o^g = N_o$  and  $N_g^g = N_g$ ,  
leading to the unit matrix

$$\begin{bmatrix} (\partial N_o^l / \partial N_o) & (\partial N_g^l / \partial N_o) \\ (\partial N_o^l / \partial N_g) & (\partial N_g^l / \partial N_g) \end{bmatrix} = \mathcal{I} \quad (49)$$

### 6.2. Two hydrocarbon phase state

Considering a control volume with both oil and gas phases present, the partial derivatives may be expressed in terms of bubble,  $\beta(p^w, T)$ , and dew point,  $\alpha(p^w, T)$ ,

$$\alpha = \frac{N_o^g}{N^g}, \quad \beta = \frac{N_o^o}{N^o}, \quad N^g = N_o^g + N_g^g, \quad N^o = N_o^o + N_g^o \quad (50)$$

In order to simplify the calculations it will be useful to introduce the molar fraction of oil phase in the system

$$z^o = \frac{N^o}{N}, \quad N = N_o + N_g = N^o + N^g \quad (51)$$

and the molar fraction of oil component  $z_o = N_o/N$ . Besides,  $z_o$  and  $z^o$  may also be expressed in terms of the bubble and dew points since

$$z_o = \frac{N^o\beta + N^g\alpha}{N} \quad (52)$$

and it is a straight forward computation to check that

$$\frac{N^o}{N} = \frac{(N^o\beta + N^g\alpha)/(N) - \alpha}{\beta - \alpha}$$

the left hand side of which is  $z^o$ , as given in (51), and substituting (52) in the right hand side gives the desired expression

$$z^o = \frac{z_o - \alpha}{\beta - \alpha} \quad (53)$$

Once the variables  $\alpha$ ,  $\beta$ , have been defined, it is necessary to give a suitable expression of the quantities to differentiate

$$\begin{aligned} N_o^o &= \beta N^o = \beta z^o N, & N_g^g &= (1 - \alpha) N^g = (1 - \alpha)(1 - z^o) N \\ N_o^g &= \alpha N^g = \alpha(1 - z^o) N, & N_g^o &= (1 - \beta) N^o = (1 - \beta) z^o N \end{aligned} \quad (54)$$

The calculation of the derivatives for (54) with respect to either the oil molar mass or the gas molar mass is now a straightforward task after substituting  $z^o$  for its corresponding value as given in (53) and recalling from  $z_o = N_o/N$  that

$$\frac{\partial z_o}{\partial N_o} = \frac{1 - z_o}{N}, \quad \frac{\partial z_o}{\partial N_g} = \frac{-z_o}{N}$$

To simplify the description, a sketch of these analytical derivatives follows:

$$\begin{aligned} \begin{bmatrix} \frac{\partial N_o^o}{\partial N_o} & \frac{\partial N_o^o}{\partial N_g} \\ \frac{\partial N_o^g}{\partial N_o} & \frac{\partial N_o^g}{\partial N_g} \end{bmatrix} &= \begin{bmatrix} \frac{(1-\alpha)\beta}{\beta-\alpha} & \frac{(1-\alpha)(1-\beta)}{\beta-\alpha} \\ -\frac{\alpha\beta}{\beta-\alpha} & -\frac{\alpha(1-\beta)}{\beta-\alpha} \end{bmatrix} \\ \begin{bmatrix} \frac{\partial N_g^o}{\partial N_o} & \frac{\partial N_g^o}{\partial N_g} \\ \frac{\partial N_g^g}{\partial N_o} & \frac{\partial N_g^g}{\partial N_g} \end{bmatrix} &= \begin{bmatrix} -\frac{\alpha(1-\beta)}{\beta-\alpha} & -\frac{(1-\alpha)(1-\beta)}{\beta-\alpha} \\ \frac{\alpha\beta}{\beta-\alpha} & \frac{(1-\alpha)\beta}{\beta-\alpha} \end{bmatrix} \end{aligned} \tag{55}$$

It is easy to verify these calculations since the sum of the two matrices above is the identity matrix, as it should be.

### 7. NUMERICAL EXAMPLES

This section will illustrate with two different examples the efficiency of the two novel implicit molar mass formulations: full Jacobian and sequential Jacobian, within the Athena simulator. As expected, it will be seen that the new implicit formulations are particularly useful to avoid the time step constraints that the CFL condition imposes when using the explicit formulation. Additionally, the robustness of the implicit methods as function of the time step will be studied.

#### 7.1. A first example: The dome

Before proceeding with the numerical experiments, the geological domain and boundary conditions shall be described. The three dimensional domain has 50 m depth on the ends, and a size of 1000 m × 100 m × 70 m. There are four different layers in the z direction: shale, sandstone, shale and sandstone again. The lithology for the sandstone has a porosity of  $\phi = 0.5$  and a permeability of  $K_x = 500$  mD,  $K_y = 500$  mD and  $K_z = 500$  mD while the corresponding values for the shale are  $\phi = 0.5$  and  $K_x = 5 \times 10^{-6}$  mD,  $K_y = 5 \times 10^{-6}$  mD and  $K_z = 5 \times 10^{-6}$  mD. The boundary conditions consist of an explicitly given flux of oil and gas with value  $5 \times 10^{-5}$  mol/m<sup>2</sup> s going inwards on the left hand side and an outwards water flux with value  $6.5 \times 10^{-4}$  mol/m<sup>2</sup> s in the right hand side. There are also temperature boundary conditions of 450 K at the top and 460 K at the bottom. The domain is uniformly subdivided in each direction as is shown in Plate 1, which serves as an illustration of the Athena output.

In order to validate the two new implicit methods for the molar mass equations, they will be compared to the explicit solver. The Athena simulator is run for each of these three methods and the time step has been set to be small enough for the CFL condition to remain inactive in the explicit case. For these small time steps the reference solution given by the explicit solver is graphically indistinguishable from the solution obtained with the implicit methods. Thus, the relevant factor to analyse is how the solution of the implicit formulation varies as the maximum allowed time step increases. Given an implicit solver, we shall compare the hydrocarbon saturations,  $S^l$ ,  $l = o, g$ , that result from simulations with different maximum

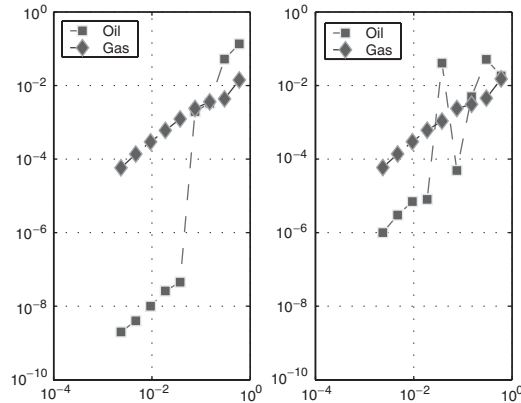


Figure 1. Athena simulation of 100y; full Jacobian solution to the left and sequential Jacobian to the right. The  $L_1$  error in saturations, against maximum allowed time step.  $\Delta t \in (0.00235y, 0.6y)$ .

Table I. CPU time statistics in seconds: Athena simulation of 100y with three different solvers.

Max. time step (y)	0.0094	0.0188	0.0376	0.0752	0.15	0.3	0.6
Explicit	2101.89	1361.75	1052.35	1127.57	941.82	1149.89	1126.96
Seq (Implicit)	1595.27	828.85	420.87	224.36	107.49	46.56	28.78
Jac (Implicit)	1628.67	822.07	413.97	208.52	98.56	42.87	26.95

value of the time steps. The error norm is chosen to be  $\|S_{\Delta t}^l - S_{\Delta t_0}^l\|_{L_1}$  with time steps,  $\Delta t$ , that double from  $\Delta t = 0.00235y$  until  $0.6y$  using as reference solution,  $S_{\Delta t_0}$ , the one obtained with maximum time step  $\Delta t_0 = 0.0006y$ . Figure 1 shows that the full Jacobian is more robust than the sequential method as it should be expected, since in the sequential formulation the cross derivatives have been neglected. Even when the error is bounded below 10%, the sequential formulation shows an erratic convergence rate for time steps bigger than  $0.0376y$  where, according to Table I, the explicit method would impose severe CFL conditions.

Concerning the computational time, it may be read in Table I not only that the implicit solvers are competitive at small time steps, which may of course be due to implementation dependent factors, but that whilst the CPU time for the explicit method remains bounded above a quantity close to that obtained when the CFL condition becomes for the first time active, the CPU time for both implicit methods decreases at a rate inversely proportional to the maximum allowed time step.

## 7.2. A highly non-linear model

In this subsection numerical results for a full 3D treatment of a domain with a fault shall be described. The domain has a size of  $[8.75, 1, 8.75] \text{ m} \times 10 \text{ m} \times [7.5, 2.5, 10] \text{ m}$  and 8 m depth at the left end. It has three different layers both in the  $x$  and in the  $z$  direction, shale, sandstone and shale again. The lithologies have the same values as those given in Section 7.1 and the boundary conditions consist of an explicitly given flux of oil and gas with value

Table II. CPU time statistics in seconds: Athena simulation of 20y with three different solvers.

Maximum time-step ( $\gamma$ )	0.00235	0.0047	0.0094	0.0188	0.0376	0.0752	0.15
Explicit	1591.09	743.04	415.31	556.41	591.16	592.15	596.06
Seq (Implicit)	1073.7	540.66	235.7	138.72	84.42	46.62	24.58
Jac (Implicit)	1175.85	542.55	241.8	131.12	77.75	41.48	23.01

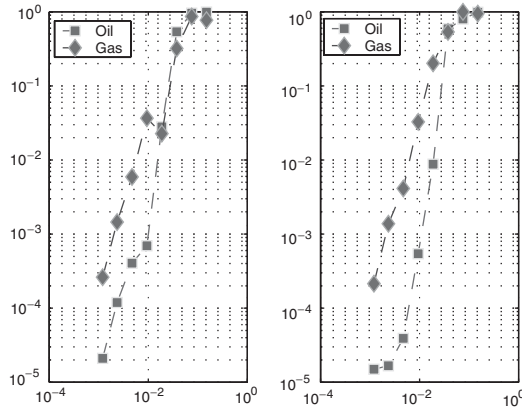


Figure 2. Athena simulation of 100y; full Jacobian solution to the left and sequential Jacobian to the right. The  $L_1$  error in saturations, against maximum allowed time step,  $\Delta t \in (0.0012y, 0.15y)$ .

$0.2 \times 10^{-4} \text{ mol/m}^2 \text{ s}$  going inwards on the left hand side and an outwards water flux with value  $2.5 \times 10^{-4} \text{ mol/m}^2 \text{ s}$  on the right hand side. Some results of this model simulation with Athena are shown in Plate 2. In this particular example the system is highly non-linear, so that the Jacobian variation at each *Newton-GMRES* step is very high, and the implicit methods can just be run with a time step about 25 times bigger than the one the CFL condition would have imposed in the explicit, as may be seen from Table II, while in the simpler case of Section 7.1 was almost 50 times bigger.

According to Figure 2, the relation between the oil and gas saturation  $L_1$ -error,  $\|S_{\Delta t}^l - S_{\Delta t_0}^l\|_{L_1}$ , and the time step for both implicit methods, allow us to conclude that, even when the discrete treatment of cross derivatives yields a natural time step control in the *Newton-GMRES*, further improvements should be introduced in order to treat regions where the phase and velocity are subject to rapid changes. As a step in that direction, a local time domain gridding and parallel processing is currently under study.

### 8. CONCLUSIONS

We apply numerical techniques to determine the essential dynamical behavior of two novel implicit formulations for the molar masses in multicomponent, multiphase flux in porous media. The Jacobian resulting from the *Newton-Rapson* algorithm is approximated analytically

from the dew an bubble point curves. The results indicate that the size of the cross-diagonal terms in the Jacobian serve as a time step control.

Moreover it can be shown that for regions where the change in velocity and phase is small, the implicit formulation performs at least a factor of 50 times faster. Hence, altogether we may conclude that both the implicit formulations for the molar mass of multicomponent, multiphase porous media exhibit a much better CPU time than the explicit solver at any time step. Besides, the error remains bounded when using a discretization-derived time step control. Some animations of these results may be found at the home-pages of the authors.

## REFERENCES

1. Øye GÅ, Reme H. Parallelization of a compositional simulator with a Galerkin coarse/fine method. In: *Euro-Par'99*, Amestoy P and others (eds). Springer: Berlin, 1999, vol. 1685; 586–594.
2. Reme H, Øye GÅ. Use of local grid refinement and a Galerkin technique to study secondary migration in fractured and faulted regions. *Computing and Visualization in Science* 1999; **2**(2/3):153–162.
3. Qin G, Wang H, Ewing RE, Espedal MS. Numerical simulation of compositional fluid flow in porous media. In *Numerical treatment of multiphase flows in porous media* Chen Z, Ewing RE, Shi ZC (eds). Springer: Berlin, 2000; vol. 552; 232–243.
4. Ewing RE, Chen Z, Qin G. Analysis of a compositional model for fluid flow in porous media. *SIAM Journal of Applied Mathematics* 2000; **60**:747–777.
5. Aavatsmark I, Barkve T, Bøe Ø, Mannseth T. Discretization on unstructured grids for inhomogeneous, anisotropic media. Part I: derivation of the methods. *SIAM Journal on Scientific Computing* 1998; **19**(5): 1700–1716.
6. Aavatsmark I, Barkve T, Bøe Ø, Mannseth T. Discretization on unstructured grids for inhomogeneous, anisotropic media. Part II: discussion and numerical results. *SIAM Journal on Scientific Computing* 1998; **19**(5):1717–1736.
7. Childs C, Sylta Ø, Moriya S, Walsh JJ, Manzocchi T. A method for including the capillary properties of faults in hydrocarbon migration models. *Norwegian Petroleum Society*, Special Publication No. 11, Hydrocarbon Seal Quantification, 16–18 October 2002, Stavanger, Norway.
8. Fladmark GE. In *Secondary Oil Migration. Mathematical and Numerical Modeling in SOM Simulator*, vol. R-077857. Norsk Hydro (eds). Bergen, 1997.
9. Lehnhäuser T, Schäfer M. Improved linear interpolation practice for finite-volume schemes on complex grids. *International Journal for Numerical Methods in Fluids* 2002; **38**(7):625–645.
10. Dogru AH, et al. A parallel reservoir simulator for large-scale reservoir simulation. *Society of Petroleum Engineers Reservoir Engineering* 2002; **5**(1):11–23.
11. Sylta O. Modeling of secondary migration and entrapment of multicomponent hydrocarbon mixture using equation of state and ray-tracing modeling techniques. In *Petroleum Migration* England WA, Fleet AJ (eds). Special Publications of the Geological Society: London, 1991; 111–122.
12. Mohamed Chaib, Gunnar E Fladmark, Magne Espedal. Implicit treatment of molar mass equations in secondary oil migration. *Comput. Visual. Sci.* 2002; **4**(3):191–196.
13. Stefania Bellavia, Benedetta Morini. A globally convergent Newton-GMRES subspace method for systems of nonlinear equations. *SIAM Journal on Scientific Computing* 2001; **23**(3):940–960.
14. Peter N Brown, Youcef Saad. Hybrid Krylov methods for nonlinear systems of equations. *SIAM Journal on Scientific and Statistical Computing* 1990; **11**(3):450–481.
15. Rémi Choquet, Jocelyne Erhel. Newton-GMRES algorithm applied to compressible flows. *International Journal for Numerical Methods in Fluids* 1996; **23**(2):177–190.
16. Thomas H Armin, Kauerauf I. Using flash calculations to determine phase composition and properties in petroleum systems modeling. *2001 Annual Conference of the International Association for Mathematical Geology*, Cancun 2001.
17. Elewaut EFM. Secondary Oil Migration Project, An integrated Geochemical and Quantitative Modeling Approach for Understanding and Predicting Secondary Oil Migration. *Technical Report*, Netherlands Institute of Applied Geoscience-TNO, National Geological Survey, December 1996.
18. Borge H. Modeling generation and dissipation of overpressure in sedimentary basins: An example from the Halten Terrace, offshore Norway. *Marine and Petroleum Geology* 2002; **19**(3):377–388.
19. Sylta Ø, Krokstad W. Prediction of Oil and Gas Column Heights in Prospects Using Probabilistic Basin Modeling Methods. *APG Annual Meeting: New Insights Into the Origin, Migration and Alteration of Petroleum*, 2001.
20. Hustad OS. A coupled model for three-phase capillary pressure and relative permeability. (*SPE Journal*) Presented at the *2000 SPE Annual Technical Conference and Exhibition*, Dallas, Texas, USA, 1–4 October 2000.

21. Slodička M. A robust and efficient linearization scheme for doubly nonlinear and degenerate parabolic problems arising in flow in porous media. *SIAM Journal on Scientific Computing* 2002; **23**(5):1593–1614.
22. Qin G. Numerical solution techniques for a compositional model. *Ph.D. Dissertation*, Department of Chemical and Petroleum Engineering, University of Wyoming, Laramie, WY, 1995.
23. Chen Z, Ewing RE. Comparison of various formulations of three-phase flow in porous media. *Journal of Computational Physics* 1997; **132**:362–373.
24. Leibovici C, Erling H. Stenby, Kim Knudsen. A consistent procedure for pseudo-component delumping. *Fluid Phase Equilibria* 1996; **117**:225–232.
25. Leibovici C, Barker J, Waché D. Method for delumping the results of compositional reservoir simulation. *Society of Petroleum Engineers Journal* 2000; **5**(2):227–235.
26. Durlofsky LJ, Chien MC. Development of a mixed finite element based compositional reservoir simulator. *SPE* 25253. *12th SPE Symposium on Reservoir Simulation*, New Orleans, LA, 1993: 221–231.
27. Watts JW. A compositional formulation of the pressure and saturation equations. *Society of Petroleum Engineers Journal* 1986; 243–252.
28. Vovelle J. Convergence of finite volume monotone schemes for scalar conservation laws on bounded domains. *Numerical Mathematics* 2002; **90**(3):563–596.

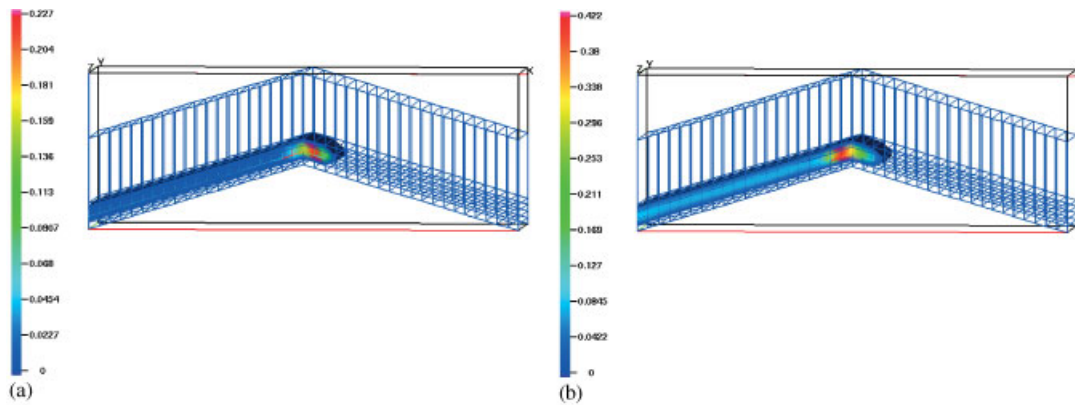


Plate 1. Hydrocarbon migration simulated by Athena for 100y with 0.0047y as time step: (a) Gas saturation; and (b) oil saturation.

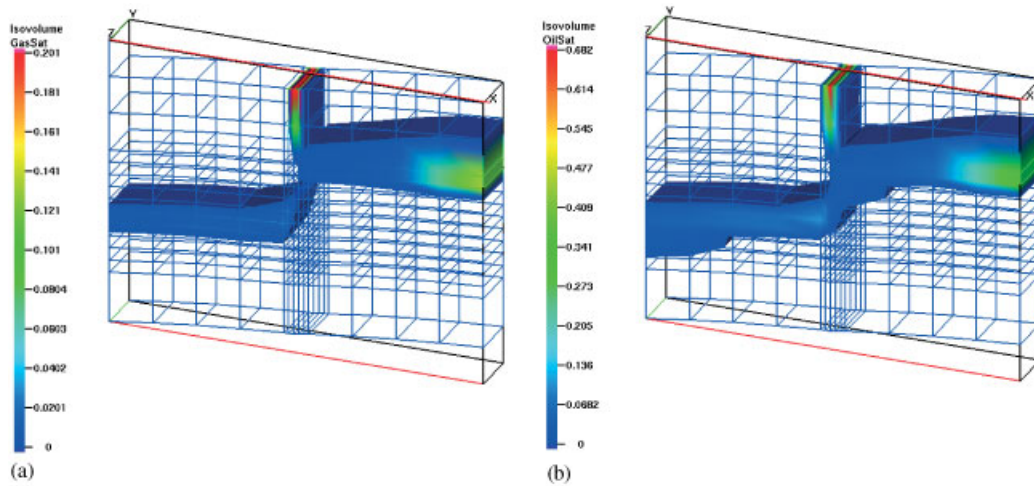


Plate 2. Hydrocarbon migration simulated by Athena for 20y with 0.0047y as time step: (a) Gas saturation; and (b) oil saturation.